Direct measurement of transversely isotropic DNA nanotube by force–distance curve-based atomic force microscopy

Zhipeng Ma[1], Young-Joo Kim[2], Seongsu Park[1], Yoshikazu Hirai[1], Toshiyuki Tsuchiya[1], Do-Nyun Kim[2], Osamu Tabata[1]

[1]*Department of Micro Engineering, Kyoto University, Kyoto 615-8540, Japan*
[2]*Department of Mechanical and Aerospace Engineering, Seoul National University, Seoul 151-744, Republic of Korea*
E-mail: z_ma@nms.me.kyoto-u.ac.jp

Published in Micro & Nano Letters; Received on 7th May 2015; Revised on 15th July 2015; Accepted on 16th July 2015

DNA origami is one of the most promising ways to create novel two-dimensional (2D) and 3D structures, assemble inorganic and organic materials, and synthesise functional micro/nano systems. In particular, DNA origami structures consisting of nanotube configurations can function as mechanical components for encapsulating materials such as gold particles or drug proteins, due to their tubular structure, relatively high rigidity, high aspect ratio and other desirable characteristics, but certain mechanical properties such as radial rigidity have yet to be fully determined experimentally. A report is presented on the direct measurement of the radial modulus of a DNA nanotube structure by force–distance curve-based atomic force microscopy, in a magnesium ion solution. A Hertz model, corrected using the finite-element method to achieve greater realism, was employed to determine the DNA nanotube's actual radial modulus in two states, corresponding to the rigidity of a porous and electrostatically repulsive nanotube lattice, and the rigidity of a packed and elastic honeycomb lattice. Furthermore, the biphasic radial modulus was verified by estimation of the inter-helix electrostatic force and torsional rigidity of a six-helix DNA nanotube, with results comparable to those reported elsewhere. The anisotropy of the DNA nanotube honeycomb lattice revealed by the authors' radial measurements should be useful when developing new DNA structures and may enable further applications that utilise DNA origami structures as a mechanical component.

1. Introduction: DNA origami [1], typically formed from a scaffold of a long strand of DNA such as M13mp18, with the help of about 200 designed single-strand DNA (ssDNA) 'staples', is a versatile methodology that facilitates the creation of nanostructures made of diverse materials; the DNA is used as an engineering material [2]. DNA origami-based nanostructures can be spatially addressable to sub-nanometre precision, enabling nanoscale materials to be deployed at particular locations. This is achieved by utilising the base sequence data of the scaffold as an address to specifically conjugate a complementary ssDNA unit that has a nanomaterial attached at the other end [2–3]. This feature of DNA origami bridges the gap between nanoscale materials and micrometre-scale devices such as MEMS/LSI, and facilitates the creation of functional micro/nanosystems that rely on phenomena specific to nanostructures, such as plasmonic effects arising from nanoparticles in close proximity [4–7]. To achieve accurate and reliable positioning of other materials in a DNA origami structure, its structural stiffness, as well as the strength of the forces by which other materials are attached or encapsulated, need to be quantitatively estimated and measured.

Among a variety of DNA origami structures, the nanotube configuration formed by parallel double-strand DNA (dsDNA) bundles arrayed in a honeycomb lattice (DNA nanotube, hereafter), is very attractive as a structural building block. DNA nanotubes can function as a versatile platform for the creation of new structural systems, by confining or encapsulating different nanoscale materials such as nanoparticles [8–9], reactive proteins and drugs [10], owing to their hollow structure, relatively high rigidity, high aspect ratio and other useful properties. However, the exploitation of DNA nanotubes as building blocks for nanostructures, and the design of nanostructures that provide specific mechanical performances, depends on a comprehensive understanding of their mechanical properties. Although studies of certain mechanical properties of dsDNA, such as its persistence length, have been carried out, there are few studies pertaining to the mechanical modelling and measurements of certain key mechanical properties of DNA nanotube structures [11–12]. Most measured results for the bending rigidity or bending persistence length of DNA nanotubes agree well with values estimated using a simple beam model in which parallel dsDNA bundles, connected continuously and rigidly, are regarded as elastic and isotropic rods having the same Young's modulus or bending persistence length as those of dsDNA (260 MPa and 50 nm, respectively) [13]. On the other hand, the measured results for torsional parameters are far below the estimated values obtained using the same beam model [13].

One explanation for the disparity between torsional parameter estimations and measurement results is that the constraints applied at the dsDNA rod connections are overly idealised, and should be discrete at crossover positions [13]. Another possible explanation for this discrepancy is to assume that the longitudinal and radial mechanical properties of a DNA nanotube are anisotropic. We consider this to be a reasonable assumption, based on the fact that the DNA nanotube is a porous biphasic material, with a designed degree of porosity and the existence of inter-helix spacing between dsDNA units, but it has yet to be experimentally verified. Therefore, further studies on the mechanical properties of DNA origami, especially the radial modulus of DNA nanotubes, are desirable.

In our previous research [14], direct quantitative measurement of the radial behaviour of a DNA nanotube was carried out, using force–distance curve-based atomic force microscopy (AFM), to determine the radial modulus of a DNA nanotube and assess the validity of the anisotropy assumption mentioned above. In addition to providing high-resolution images of DNA nanotube surfaces, the AFM system was utilised to probe mechanical properties, by measuring the mechanical response of a DNA nanotube as the AFM cantilever is indented into it and withdrawn.

In this Letter, the structure of a newly designed DNA nanotube is presented first. Next, we discuss the method for measuring the radial modulus of the DNA nanotube, based on AFM force–distance curves obtained with the sample immobilised on a mica surface in a magnesium ion solution. A Hertz model, corrected

with the finite-element method (FEM) to obtain increased realism, is then used to determine the biphasic radial modulus of the DNA nanotube, based on the measured force–distance curves. Finally, a biphasic radial modulus was obtained for the DNA nanotube in two applied force regimes: we termed the modulus obtained in the low applied force state the radial electrostatic modulus, and that in the high force state the radial elastic modulus. To verify these data, we first estimated the electrostatic force acting on DNA helices in a honeycomb lattice and found that the electrostatic osmotic pressure estimated from the radial electrostatic modulus is very comparable to that for DNA helices in a hexagonal lattice in a similar magnesium ion solution reported elsewhere [15]. In addition, we constructed a new transversely isotropic model for typical DNA nanotubes in a honeycomb lattice in which the torsional rigidity is determined from the radial elastic modulus measured in our study. The torsional persistence of a six-helix DNA nanotube estimated from this new model agrees well with that reported elsewhere.

2. Methods: The DNA nanotube employed in our experiments was designed with caDNAno software and its shape and structure were verified with CanDo software [16]. As shown in Fig. 1*a*, the scaffold is aligned into a honeycomb lattice formed by 24 parallel dsDNA bundles. The length and diameter of the DNA nanotube are estimated as roughly 100 and 12 nm, respectively (Fig. 1*b*), and AFM imaging verifies these approximate dimensions. The

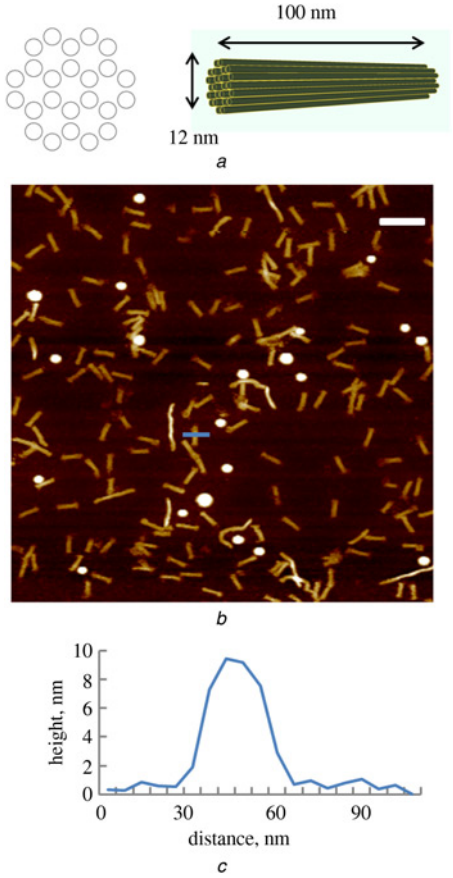

Figure 1 *Schematic configuration and AFM image of the designed DNA nanotubes*
a Schematic view of DNA nanotube three-dimensional structure (right), with a cross-section showing the honeycomb lattice (left)
b AFM image of DNA nanotubes deposited on mica substrate
c Cross-sectional profile of one DNA nanotube indicated by the blue line in Fig. 1*b*, in which the measured height is a little bit smaller than the designed diameter of a DNA nanotube because of the deformation occurred during the measurement process

nanotubes are straight and of uniform length, which indicate that the regular distribution of nicks and crossovers has prevented the concentration of stress. A quantity of the designed DNA nanotube was produced by mixing the M13mp18 scaffold (New England Biolabs, Japan) with 179 different synthesised staples (Eurofins Genomics, Japan) at a 1:10 ratio, that is, one copy of the scaffold strand to ten copies of staple strands. The mixture containing 10 nM of scaffold DNA and 100 nM of each staple DNA dispersed in a buffer solution (5 mM TRIS-HCL, 1 mM EDTA and 14 mM $MgCl_2$) was subjected to a standard thermal protocol in which the mixture was rapidly heated to 80°C and then cooled to 60°C at a rate of 4 min/°C, then cooled to 24°C at a rate of 120 min/°C. The assembled DNA nanotubes were purified by centrifuging with an Amicon Ultro-0.5 ml centrifugal filter (100 kDa) to remove excess staple DNA material and then stored at 4°C for later use. Prior to AFM measurements, the prepared DNA nanotube solution was further diluted 1:4 with the same buffer solution and then deposited during a 5 min interval on a freshly cleaved mica surface pre-treated with $NiCl_2$. After the application, the mica surface with the sample was washed with deionised water twice. The mica surface and cantilever cell were wetted with a buffer solution before indentation measurements were carried out.

A commercial AFM (Multimode 8, Veeco, USA) was used in quantitative nanomechanical property mapping mode to obtain force–distance curve measurements, with each pixel representing a 1 × 1 nm area. To ensure the fixation of DNA nanotube structures on the mica surface, the same surface with dispersed DNA nanotube structures were scanned for several cycles and all DNA nanotubes still existed on the mica surface with structural integrity. A triangular cantilever probe with a nominal spring constant of 0.4 N/nm, nominal resonant frequency of 70 kHz and nominal tip radius of 2 nm was used to ensure reproducible results. The deflection sensitivity of the cantilever was determined by measuring vertical displacements towards the mica surface, with minimal force applied before and after each measurement. The spring constant of the cantilever was obtained by analysing thermal noise, using the thermal tuning protocol provided in the Nanoscope Analysis software. The tip radius of the cantilever probe was estimated with a relative method based on a PDMS reference sample with a nominal Young's modulus of 3 MPa. The frequency of the current applied to the piezoelectric cantilever actuator moving the probe towards and away from the samples surface was set to 2 kHz and the maximum force was kept below 1.5 nN, to ensure that the cantilever tip did not destroy the DNA nanotube samples.

A Hertz model was corrected to improve the determination of the radial modulus of the DNA nanotube via the measured indentation force curves. In this model, the DNA nanotube and cantilever tip are approximated as a cylindrical beam and sphere, respectively, and their relationship is expressed in (1), where F and δ are the force and indentation distance, respectively, E is the Young's modulus, σ is the Poisson's ratio and R_e is the effective radius, which depends on the values of the tip radius (R_t) and tube radius (R_c). In this work, a Poisson's ratio of 0.5 for the DNA nanotube was assumed. This Hertz model is widely accepted as a mathematical model for load-deformation behaviour during elastic contact, and obtains the elastic rigidity under the assumption of small strains at the contact region, with strains beyond this region disregarded [17]

$$F = \frac{4}{3}\left(\frac{E}{1-\sigma^2}\right)\sqrt{R_e}\delta^{3/2} \tag{1}$$

where

$$R_e = \sqrt{\frac{R_t^2 R_x}{R_t + R_c}}$$

To minimise errors caused by the above assumption, a FEM can be used to correct the mathematical model expressed in (1). In this

doi: 10.1049/mnl.2015.0174

research, ANSYS 14.5 software was employed to solve the contact problem, with the DNA nanotube, cantilever tip and mica substrate modelled as a cylinder with isotropic elasticity, a rigid sphere and a rigid flat plane, respectively. For simplicity, no initial deformation of the DNA nanotube or mica surface was assumed. The viscoelastic effect due to the surrounding ionic fluid environment was neglected in our model. To reduce computational time, a quarter-symmetric model with corresponding symmetric boundary conditions was used.

A correction factor, f, was introduced in the corrected Hertz model to ensure adequate agreement between the results of measurements using the mathematical model and simulated results. As shown in Fig. 2, the corrected Hertz model expressed in (2) can predict simulation results more accurately than the original Hertz model (1). Equation 3 shows the corrected Hertz model with the addition of a contact point, with F_0 and δ_0 representing new origins for the force and distance, respectively. The dependency of the correction factor on the probe tip radius is shown in Fig. 3 and estimated using the fitted second-order polynomial equation of (4) for the analysis of the radial modulus. The calibrated tip radius ranged from 5 to 10 nm for the cantilever we chose, larger than the nominal value of 2 nm, possibly due to mechanical wear during the calibration and scanning processes

$$F = \frac{4}{3}\left(\frac{Ef}{1-\sigma^2}\right)\sqrt{R_e}\delta^{3/2} \tag{2}$$

$$F - F_0 = \frac{4}{3}\left(\frac{Ef}{1-\sigma^2}\right)\sqrt{R_e}(\delta - \delta_0)^{3/2} \tag{3}$$

$$f = -0.001R_t^2 + 0.027R_t + 0.633 \tag{4}$$

3. Results and discussion: Fig. 4 shows typical force–distance curves for the centre of the DNA nanotube immobilised on the mica surface since the DNA nanotube is fixed stably under the compression of the cantilever tip near the centre and the contact problem can be simply assumed as a contact without separation and a slide between the DNA nanotube and the mica surface. The loading curve determined for the mica surface alone is used to alert us to whether the cantilever tip is responding to the underlying mica surface. When performing DNA nanotube measurements, this condition is recognisable in both the loading and unloading force curves when the compression force is at a high level (above about 1 nN). An accurate estimation of the elastic response of the DNA nanotube is therefore impossible in this high-force region. Furthermore, our analyses are based on unloading force curves instead of loading force curves, because the latter include plasticity and viscosity responses. Concerning the noise-force region illustrated in Fig. 4, the oscillatory vibration of the cantilever tip arises when it loses contact with the DNA nanotube sample, but this vibration is extinguished when tip re-establishes contact. This vibration is regarded as noise and can be negated by a correction process in the Nanoscope Analysis software. Ultimately, the contact point is estimated based on the zero force point obtained in the corrected force–distance curves and the error associated with this approximation is negligible for this experiment. The low-force region indicated in Fig. 4 is utilised for the analysis of the DNA nanotube radial modulus. In this low-force region, the adhesion is normally <50 pN, which is small enough to keep the DNA nanotube structures

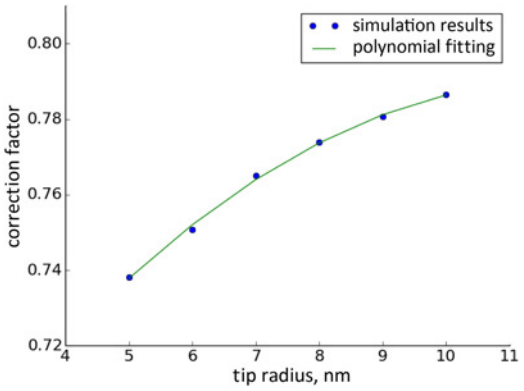

Figure 3 *Tip radius dependency of correction factor*

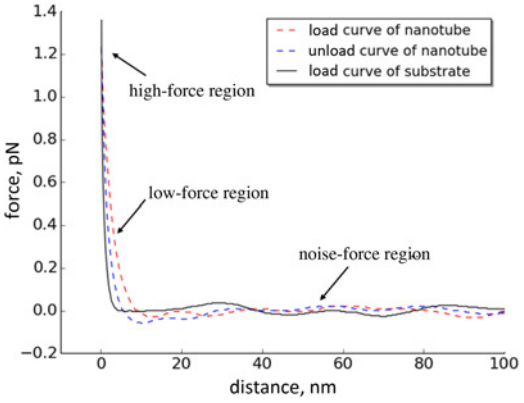

Figure 4 *Typical nanoindentation force–distance curves for DNA nanotubes on a mica substrate*

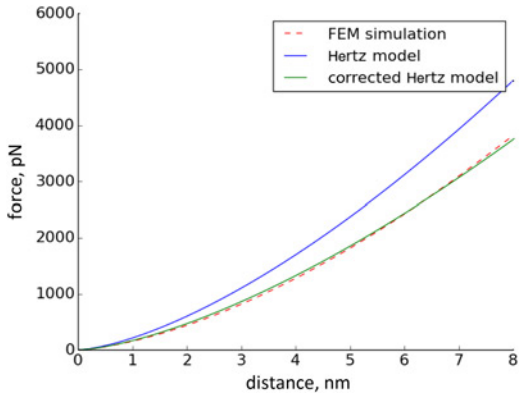

Figure 2 *Prediction of FEM simulation results by corrected Hertz model (tip radius: 9 nm, Young's modulus: 50 MPa)*

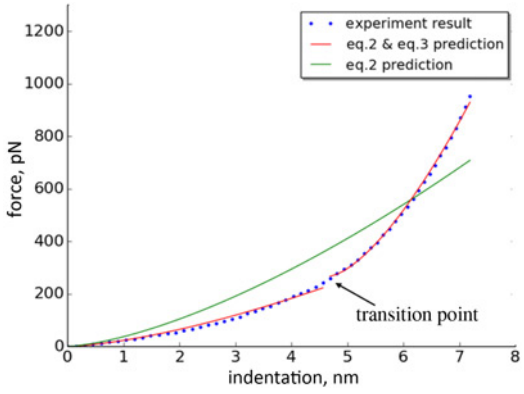

Figure 5 *Measured force-indentation data (blue dots) and fitted curves obtained by the corrected Hertz model, compared with single phase prediction (green line) and two-phase prediction (red line)*

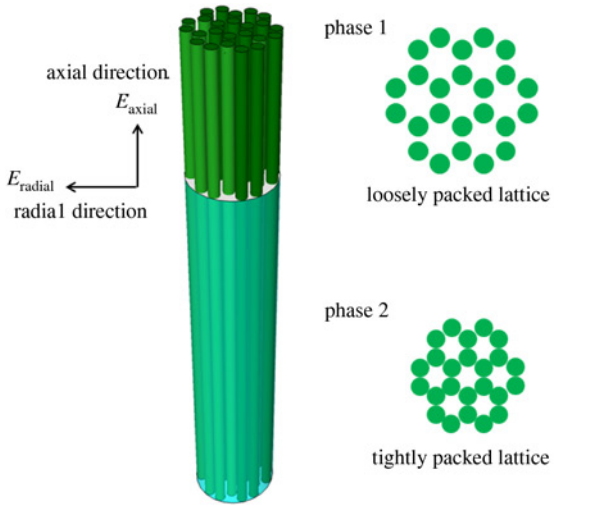

Figure 6 *Illustration of the DNA nanotube with loosely packed lattice and tightly packed lattice corresponding to two measurement phases*

intact [18]. Fig. 5 shows the force-indentation curve (blue dots) converted from the force–distance curve that is based on the determined contact point.

As mentioned above, we assume that the DNA nanotube will behave as a porous biphasic material under radial compression, as illustrated in Fig. 6. During the first measurement phase, when the applied force and deformation are both small, the DNA nanotube undergoes a reduction of inter-helix spacing between adjacent dsDNA helices, and the inherent electrostatic forces between adjacent dsDNA strands therefore dominate the response. As the compressive force is increased, evidence of a transition is expected to appear in the force-indentation curve, after most of the inter-helix space between adjacent dsDNA strands is eliminated. During the second measurement phase, when the force and deformation are both relatively large, the behaviour under compression primarily reflects the arrangement of the dsDNA bundles in a tightly packed lattice.

On the basis of the assumption that the material property being investigated here is biphasic, the force-indentation curves were fitted using the two integrated corrected Hertz models expressed in (2) and (3) for the two measurement phases with origin points at (0, 0) and (F_0, δ_0), respectively. The corrected Hertz model with an origin point at (0, 0) expressed in (2) was utilised to fit the force–distance curves at the low-force region, while the corrected Hertz model with an origin point at (F_0, δ_0) was for the high-force region of the force–distance curves. The process of fitting was carried out automatically by iterative searching of the minimal integral mean square error of the fitted results at two regions, illustrated in Fig. 5 by the two red lines for them. We note that the transition point indicated by the arrow in Fig. 5 does not necessarily coincide with the contact point (F_0, δ_0) included in (3), and will cause underestimated or overestimated results if chosen inaccurately. The fitted results obtained by the integrated models were in good agreement with the experimental measurements. As the green fitted line in Fig. 5 indicates, the estimation based on the singly corrected Hertz model expressed in (2) conforms poorly with the measured results.

The above fitting protocols were carried out for all force-indentation curves for different DNA nanotubes ($N = 72$), to obtain two sets of Young's modulus values for the DNA nanotube design, termed the radial electrostatic modulus for the first measurement phase, and the radial elastic modulus for the second measurement phase. The measurement results are illustrated in Fig. 7. The radial electrostatic modulus of the DNA nanotube was determined to have an average value of 11.5 MPa, with a standard deviation of 4 MPa, and the average value for the radial elastic modulus was 64.8 MPa, with a standard deviation of 21.1 MPa. Both of

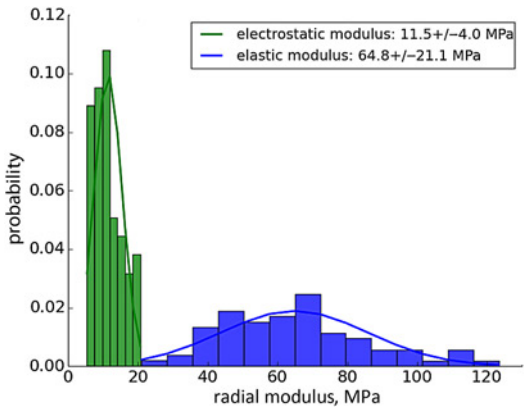

Figure 7 *Measured electrostatic and elastic moduli ($N = 72$)*

these radial modulus values are remarkably low compared with the reported Young's modulus for dsDNA of about 260 MPa [13]. Considering the reported longitudinal elastic modulus of roughly 260 MPa, our measurements indicate that the axial and radial moduli of the DNA nanotube used in this experiment are anisotropic.

To accurately verify our assumption that inter-helix electrostatic forces dominate during the first measurement phase, when both the applied force and the deformation are relatively small, we must estimate these forces, and thus the osmotic pressure of the DNA helices in the honeycomb lattice. However, accurately measuring the osmotic pressure between helices becomes increasingly complex when working with DNA nanotubes that are assembled using crossover structures. Therefore, we use the osmotic pressure values for DNA helices in the hexagonal lattice reported in [15] for comparison with the estimated value obtained from our measured radial electrostatic modulus. For simplicity, the reduction in the space between adjacent dsDNA strands as the DNA tube is deformed is presumed to follow the behaviour predicted by the Hertz model. Therefore, the average contact pressure between the cantilever tip and the DNA nanotube can be estimated from the applied compression, as expressed in (5), and equates to the mean osmotic pressure of the DNA nanotube helices

$$\int_0^{x_0} F\mathrm{d}x = \int_0^{x_0} PA\mathrm{d}x \tag{5}$$

where x is the indentation variable, x_0 the maximum indentation of the cantilever tip into the DNA nanotube, F the applied force, P the mean osmotic pressure between the cantilever tip and DNA nanotube, and A the contact area.

Assuming that the contact area can be approximated as an ellipse with an effective radius of a in the axial direction and b in the radial direction of the DNA nanotube, (6) can be derived from (5) by regarding the applied force as a function of the radial electrostatic modulus, based on the corrected Hertz model

$$\int_0^{x_0} \frac{4}{3}\left(\frac{Ef}{1-\sigma^2}\right)\sqrt{R_\mathrm{e}}x^{3/2}\mathrm{d}x = \int_0^{x_0} P\pi R_\mathrm{e}\mathrm{d}x \tag{6}$$

where $A = \pi ab = \pi R_\mathrm{e}$.

The mean osmotic pressure can then be expressed as a function of the measured radial electrostatic modulus, as formulated below

$$P = \frac{8Efd^{3/2}}{15\pi\sqrt{R_\mathrm{e}}(1-\sigma^2)} \tag{7}$$

Assuming that the indentation of 3 nm that is under the transition point between the two measurement phases, and that the measured

doi: 10.1049/mnl.2015.0174

radial electrostatic modulus has a value of 11.5 MPa, a mean osmotic pressure of about 4 MPa can be derived using (7). This derived result is comparable to the reported osmotic pressure that ranges from 1 to 3 MPa for hexagonal DNA helices in the presence of magnesium ions [15]. This implies that the radial electrostatic modulus value of 11.5 MPa that we obtained is reasonable and that the indentation behaviour during the first measurement phase is in fact dominated by electrostatic forces between the DNA helices that form the DNA nanotube.

As explained in the Introduction, the porous characteristic of DNA nanotube structures may be an alternative reason for the unexpectedly low torsional rigidity of the six-helix DNA nanotube reported in [13]. The torsional persistence length (P_t) also quantifies the rigidity in terms of twisting and can be determined from the torsional rigidity, using the following equation

$$P_t = \frac{C}{k_B T} \tag{8}$$

where k_B is the Boltzmann's constant and T is the temperature in Kelvin.

The torsional rigidity (C) of a six-helix DNA nanotube in a honeycomb lattice can also be calculated as the product of the torsion constant (J_T) for the six-helix honeycomb cross-section and the shear modulus (G), as follows

$$C = J_T G \tag{9}$$

where the torsion constant (J_T) for the six-helix honeycomb section is expressed as

$$J_T = \frac{\pi r^4}{2} \tag{10}$$

where r is the effective radius of the six-helix honeycomb lattice DNA nanotube, assumed to be 3 nm here.

Considering the longitudinal elastic modulus of about 260 MPa reported for dsDNA and other DNA nanotube structures [11], we propose a new mechanical model for such DNA nanotubes in which the radial elastic modulus is transversely isotropic, with a value of about 65 MPa, and the axial elastic modulus is roughly 260 MPa, as illustrated in Fig. 6. It is known that, for a cylindrical structure with a transversely isotropic material property, the shear modulus (G) about the tube axis can be directly determined according to the radial elastic modulus (E_{rad}), as follows

$$G = \frac{E_{rad}}{2(1+\sigma)} \tag{11}$$

Given the above relationship, the shear modulus of the six-helix DNA nanotube is calculated as 21.7 MPa, based on our measured value of 65 MPa for the radial elastic modulus. Therefore, using (12) and this radial elastic modulus, the torsional persistence length for the six-helix DNA nanotube should be 581 nm, a figure comparable to the reported value of 530 ± 20 nm [13], indicating that the 65 MPa value for the radial elastic modulus can be considered reasonable. The reason why the radial elastic modulus has a lower value than that of the longitudinal elastic modulus can be attributed to the effect of the pores inherent in the honeycomb lattice, and the grooves in the dsDNA strands

$$P_t = \frac{\pi r^2 E_{rad}}{4 k_B T (1+\sigma)} \tag{12}$$

4. Conclusion: The radial modulus of a newly designed DNA nanotube was characterised using force–distance curve measurements obtained by AFM, with the specimen in a magnesium buffer solution. Using a corrected Hertz model, biphasic mechanical properties, that is, the radial electrostatic and radial elastic moduli, were quantitatively determined to be 11.5 ± 4 and 64.8 ± 21.1 MPa, respectively. The appropriateness of these figures was verified by using them in comparisons of estimated and reported values for the inter-helix mean osmotic pressure and torsional persistence length of a six-helix DNA nanotube. We have also demonstrated the aptness of our model in which the radial elastic modulus of the DNA nanotube is transversely isotropic and much lower than that in the axial direction. In future work, we hope to develop a more precise and comprehensive model that considers the influence of much smaller features, such as the crossover and nick structures that are important aspects of DNA nanotube architecture.

5. Acknowledgments: This project was supported by JSPS and NRF under the Japan–Korea Basic Scientific Cooperation Program, and partly supported by Shaoxing 330 Plan ACY201501. Additionally, Zhipeng Ma is especially grateful for CSC scholarship support.

6 References

[1] Rothemund P.W.: 'Folding DNA to create nanoscale shapes and patterns', *Nature*, 2006, **440**, (7082), pp. 297–302
[2] Kuzyk A., *ET AL.*: 'DNA-based self-assembly of chiral plasmonic nanostructures with tailored optical response', *Nature*, 2012, **483**, (7389), pp. 311–314
[3] Jensen J.O., *ET AL.*: 'Nanoengineered bioplatforms based on DNA origami', *Proc. IEEE*, 2014, **102**, (7), pp. 1046–1049
[4] Kuzuya A., *ET AL.*: 'Nanomechanical DNA origami devices as versatile molecular sensors'. Proc. of IEEE Int. Conf. on Nano/Micro Engineered and Molecular Systems (NEMS), 2012, pp. 318–321
[5] Tabata O.: 'A closer look at DNA nanotechnology', *IEEE Nanotechnol. Mag.*, 2010, **4**, (4), pp. 13–17
[6] Akishiba T., *ET AL.*: 'DNA origami assembly on patterned silicon by AFM based lithography'. Proc. of IEEE Int. Conf. on Micro Electro Mechanical Systems (MEMS), 2013, pp. 307–310
[7] Huang C., *ET AL.*: 'Configurable assembly of DNA origami on MEMS by microfluidic device'. Proc. of IEEE Int. Conf. on Nano/Micro Engineered and Molecular Systems (NEMS), 2011, pp. 197–200
[8] Kiss S.Z., *ET AL.*: 'AuNPs conjugate DNA origami nanotubes for nanophotonic application'. Proc. of IEEE Int. Conf. on Nano/Micro Engineered and Molecular Systems (NEMS), 2012, pp. 402–404
[9] Helmi S., *ET AL.*: 'Shape-controlled synthesis of gold nanostructures using DNA origami molds', *Nano Lett.*, 2014, **14**, (11), pp. 6693–6698
[10] Jiang Q., *ET AL.*: 'DNA origami as a carrier for circumvention of drug resistance', *J. Am. Chem. Soc.*, 2012, **134**, pp. 13396–13403
[11] Rothemund P.W., *ET AL.*: 'Design and characterization of programmable DNA nanotubes', *J. Am. Chem. Soc.*, 2004, **126**, (50), pp. 16344–16352
[12] Li L., *ET AL.*: 'Manipulation of DNA origami nanotubes in liquid using tapping-mode atomic force microscopy', *Micro Nano Lett.*, 2013, **8**, (10), pp. 641–645
[13] Kauert D.J., *ET AL.*: 'Direct mechanical measurements reveal the material properties of three-dimensional DNA origami', *Nano Lett.*, 2011, **11**, (12), pp. 5558–5563
[14] Ma Z., *ET AL.*: 'Direct characterization of radial modulus of DNA nanotube by AFM nanoindentation'. Proc. of IEEE Int. Conf. on Nano/Micro Engineered and Molecular Systems (NEMS), 2015, pp. 581–584
[15] Rau D.C., Lee B., Parsegian V.A.: 'Measurement of the repulsive force between polyelectrolyte molecules in ionic solutions: hydration forces between parallel DNA double helices', *Proc. Nat. Acad. Sci. USA*, 1984, **81**, pp. 2621–2625
[16] Kim D.N., *ET AL.*: 'Quantitative prediction of 3D solution shape and flexibility of nucleic acid nanostructures', *Nucleic Acids Res.*, 2012, **40**, (7), pp. 2862–2868
[17] Shen W., Jiang B.: 'Investigation of radial compression of carbon nanotubes with a scanning probe microscope', *Phys. Rev. Lett.*, 2000, **84**, (16), pp. 3634–3637
[18] Song J., *ET AL.*: 'Isothermal hybridization kinetics of DNA assembly of two-dimensional DNA origami', *Small*, 2013, **9**, (17), pp. 2954–2959